

## **Ultra-Fast Phase-Contrast X-ray Imaging of Near-Nozzle Velocity Field of High-Speed Diesel Fuel Sprays**

Zunping Liu<sup>1</sup>, Kyoung-Su Im<sup>1</sup>, Xingbin Xie<sup>2</sup>, Yujie Wang<sup>1</sup>, Xusheng Zhang<sup>1</sup>,  
Seoksu Moon<sup>1</sup>, Jian Gao<sup>1</sup>, Kamel Fezzaa<sup>1</sup>, Ming-Chia Lai<sup>2</sup>, Kathy Harkay<sup>1</sup>,  
Vadim Sajaev<sup>1</sup>, Louis Emery<sup>1</sup>, and Jin Wang<sup>1\*</sup>

<sup>1</sup>X-Ray Science Division, Argonne National Laboratory, 9700 South Cass Ave.,  
Argonne, IL 60439-4800;

<sup>2</sup>Department of Mechanical Engineering, Wayne State University, 5050 Anthony  
Wayne Dr, Detroit, MI 48202.

### **Abstract**

High-pressure, high-speed diesel fuel sprays are complex multiphase flow phenomena. Enormous effort has been devoted to understand their dynamics that is essential to their near-nozzle breakup. In this optically dense region, conventional optical techniques are not effective to probe. By taking advantage of high-intensity and high-brilliance x-ray beams available at the Advanced Photon Source (APS), the morphology of the sprays can be imaged with x-ray phase contrast imaging and with sub-ns temporal resolution. Furthermore, a special x-ray timing mode was developed at the APS, so that two x-ray pulses with a few nanosecond width and a fixed interval of about 200 ns can be used to visualize the high-speed sprays. By tracking the movement of features in the double-exposure images without the need of seed particles, we have been able to extract velocity fields of the sprays. Velocity field is obtained by using local autocorrelation analysis of the double-exposure images of the entire sprays and during entire injection events. Two slightly different single-hole minisac nozzles were used, one with a hydroground rounded orifice inlet and the other one with a sharp inlet. In the quasi-steady state of the injection to 0.1 MPa nitrogen gas, the diesel sprays from the types of nozzles show distinct dynamic behaviors near nozzle exit, showing different velocity fields. The velocity field mapping also reveals the near-nozzle spray dynamics dependence on nozzle geometry and the injection conditions.

Key words: velocity field, diesel spray, discharge coefficient, ultrafast phase-contrast x-ray imaging

---

\*Corresponding author, wangj@aps.anl.gov

## Introduction

Understanding of the mechanism of fuel spray breakup is a key to make combustion cleaner and more efficient. Behavior of a fuel spray can be characterized through its feature morphology and velocity. Attempts to use conventional laser optical techniques to provide such information have been extensively reported in literature, but unsuccessful in the region near nozzle exit where the spray has high density and the multiple scattering by droplets and interfaces occur. X-ray technologies have been employed to measure spray mass distribution [1], record spray morphology [2, 3] and detect spray velocity [2] because of weak interaction of x-ray with matter. Time-resolved spray morphology in the region near nozzle exit is obtained by making use of image contrast from boundaries and interfaces between materials with different refraction index or abrupt thickness variations [4]. As pointed out in [3], spray behavior is dominated by upstream hydrodynamics of the spray and the surrounding gas has no effect on it before it starts to break up. In velocity measurement, the conventional techniques either need help with invasive seeding [5], or can only yield the leading-edge velocity [6]. An x-ray phase-contrast-imaging-based particle tracking velocimetry method [7] was reported for elucidating velocity fields of polydispersed particle-laden flows. The velocity in [2, 7] is less than 90 m/s, while velocity of high-pressure diesel injection is around or faster than sound speed. Using mass conservation method gives limit amount of information on the jet speed [8, 9].

This paper demonstrates that x-ray phase-contrast imaging technique is now capable to measure the velocity of diesel jets. Velocities of diesel jets at the same injection conditions but from two types of nozzles are compared. The results are also compared with results from Bernoulli equation for pipe flow.

## Experiment

The light source is the high-intensity and high-brilliance x-ray beams available at the Advanced Photon Source (APS). As shown in figure 2, a special hybrid fill pattern (1+3×7) was developed, which has 3 pulse trains of 28 mA with two 220 ns temporal gaps in between, and 1 singlet of 16 mA 1.59  $\mu$ s away from the 28 mA seplets from either size. The singlet was used to visualize morphology of diesel jets as single exposure, while two 17-ns x-ray pulses were employed in phase-contrast imaging to visualize the high-speed sprays in the optically dense near-nozzle region.

The diesel jet was injected from a common rail into a quiescent nitrogen gas ambient chamber using a common-rail injection system. Two types of nozzle, hydroground (HG) and nonground (NG) at the inlet, were used and shown in Fig. 2. A gentle nitrogen flow (at atmospheric pressure and room temperature) was

generated through a spray chamber in order to scavenge the fuel vapors. The breaking current takes 150  $\mu$ s, the holding current takes 850  $\mu$ s, and the real injection duration is around 1.6 ms for injection pressures of 50, 70, and 100 MPa.

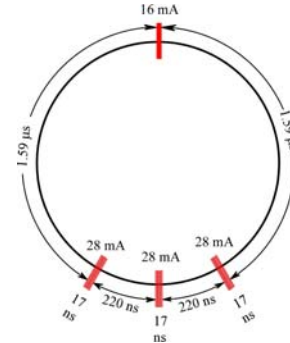


Figure 1. Hybrid fill x-ray pattern (1+3×7).

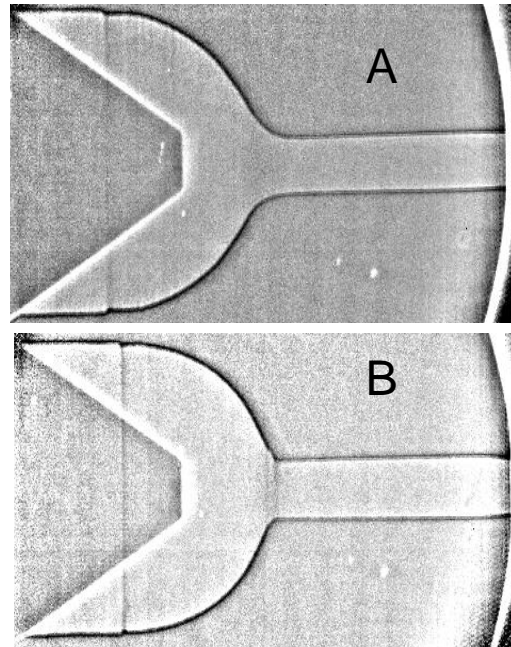


Figure 2. Internal structure of hydroground (HG) and nonground (NG) nozzles. The nominal diameters of both nozzles at exit are 180  $\mu$ m. A: HG, B: NG.

## Results and Discussion

Figure 3 shows the morphology of diesel jets at injection pressure of 50 MPa and at steady state -- 940  $\mu$ s after start of injection (ASOI). As shown in Fig.3A (single exposure), features including surface waves and ligaments are clearly visible. The image in Fig.3B was taken at the same conditions as above but with double exposures. The double-exposure image in Fig.3C is for the jet from NG nozzle. The difference between mor-

phologies of jets from HG and NG nozzles is distinctive, which is described and explained in [10].

As shown in [10], the effect that nozzle internal geometry affects jet behavior mostly occurs at steady state of injection. Therefore, velocity measurement in this work focuses at steady state. The vertical red dash line in B and C indicates positions for velocity measurement in this paper. Choose a small window of  $57 \times 249$  pixels ( $0.67 \mu\text{m}/\text{pixel}$ ) with center at a desired location of a double-exposure image, apply autocorrelation -- the cross-correlation of a signal itself -- to the window, summarize the resultant matrixes of autocorrelation at the same location of all images of the same conditions, and illustrate the final autocorrelation function in Fig. 4A. The two peaks in line-cut of autocorrelation correspond to two overlapping spray positions, so that the velocity can be calculated with temporal gap 220 ns.

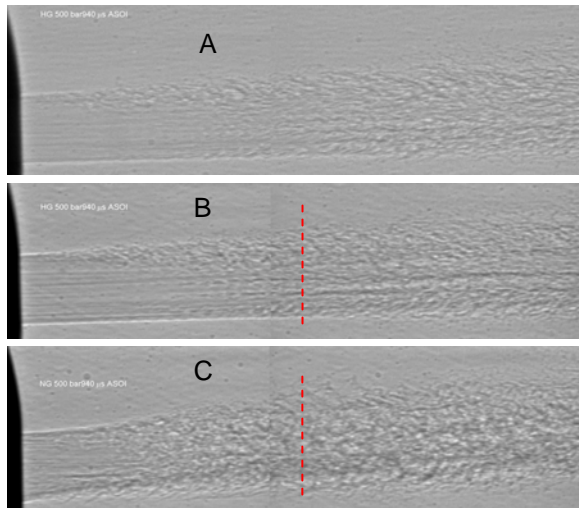


**Figure 3.** Example Morphology of diesel jets at 50 MPa injection pressure and at steady state (940  $\mu\text{s}$  ASOI). A: single exposure of jet from HG nozzle. B: double exposure of jet from HG nozzle. C: double exposure of jet from NG nozzle. Each image is composed from two individual pictures at corresponding positions, indicated by a vertical stitch line. The nominal diameters of both nozzles are  $180 \mu\text{m}$ . The vertical red dash line in B and C indicates positions for velocity measurement in this paper.

Velocity vectors are illustrated in Fig. 5. The velocity field of each jet shows maximum value at center of jet and decreasing value toward jet edges. Comparing velocity fields at each injection pressure, the vertical component of velocity of jets from NG nozzle is generally larger than that from HG nozzle. Also, the jets from NG nozzle are wider than that from HG nozzle. In other words, the velocity fields show that jets

from NG nozzle is more dispersive than that from HG nozzle.

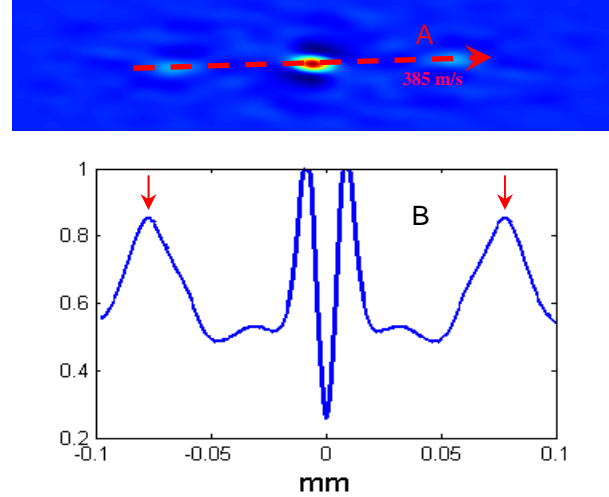


**Figure 4.** Autocorrelation function and velocity. A: autocorrelation function and velocity, B: normalized intensity profile of line-cut of autocorrelation function. The two peaks indicated by red arrows correspond to the overlapping sprays from either direction. The velocity is calculated based on the peak positions in the autocorrelation function.

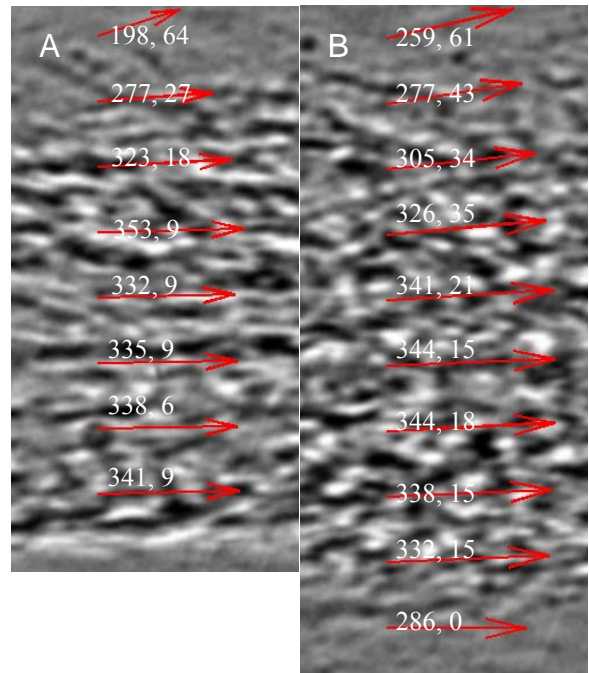


**Figure 5.** Illustration of velocity vectors of jets at position of 1.5 mm from nozzle tips. The red arrows indicate velocity vectors by length for magnitude and direction for direction. A: 50 MPa injection pressure and HG nozzle, the velocity vectors are expressed as  $V_x$  and  $V_y$  (m/s), B: 50 MPa and NG nozzle.

Velocity values are also shown Table 1. It is noticed that the maximum velocities for the same nozzle do not always appear at the same position of jet. It is reasonable because the velocity measurement is based on features that are captured and distinguishable during autocorrelation progress. The results from Bernoulli equation for pipe flow, Eq.1, are also put in Table 1,

$$V_2 = \sqrt{\frac{2(P_1 - P_2)}{\rho} + V_1^2}, \quad (1)$$

where,  $P_1$  and  $V_1$  are the pressure and velocity at inlet entrance of nozzle,  $P_2$  and  $V_2$  pressure and velocity at exit of nozzle, and  $\rho$  is the density of diesel fuel. Diesel density at room temperature is used for Table 1.

Injection pressure (MPa)		50			70			100		
Velocity from Eq.1 (density: 855.5 kg/m <sup>3</sup> )		342 m/s			405 m/s			484 m/s		
Nozzle	Position (μm)	Vx m/s	Vy m/s	Cv	Vx m/s	Vy m/s	Cv	Vx m/s	Vy m/s	Cv
HG	119									
	156	198	64		189	64		283	46	
	194	277	27		332	21		408	34	
	232	323	18		375	18		460	24	
	271	353	9	1.03	420	9		503	18	1.04
	309	332	9		426	9		503	15	
	347	335	9		414	6		499	9	
	385	338	6		423	6		487	12	
	423	341	9		429	9	1.06	493	12	
	462							414	0	
NG	119	259	61		302	67		253	70	
	156	277	43		341	52		317	30	
	194	305	34		381	46		439	52	
	232	326	30		396	34		457	40	
	271	341	21		408	24		475	30	0.98
	309	344	15		414	18		475	24	
	347	344	18	1.01	420	18	1.04	475	24	
	385	338	15		414	21		472	18	
	423	332	15		384	9		442	12	
	462	286	0		241	0		420	3	

Table 1. Velocity comparison. In the row of Bernoulli, velocity at each injection pressure is estimated by using diesel density at room temperature for both nozzles with assumptions that velocity at inlet entrance is nearly zero and pressure at nozzle exit is nearly zero. Cv is the velocity coefficient, defined as measured velocity magnitude over that from Bernoulli equation.

It is noticed that the coefficient of maximum value of experimental velocity over the one from Eq.1, defined here as velocity coefficient (Cv), is around one with error of several percentage for all injection cases. The error sources include injection pressure and density value with respect to the unknown temperature of fuel at injection. The velocity coefficient is slightly higher for HG nozzle than NG nozzle, which is reasonable because the round inlet of HG nozzle has less affect to the flow than the sharp inlet of NG nozzle.

With the direct measurement of the near-nozzle jet velocity, we should now to exam the concept of the so called “discharge coefficient” and its implication on the velocity. The discharge coefficient, Cd, is defined as ratio of actual mass flow over ideal mass flow of a spray [11]. It is an engineering coefficient sometimes calculated as the product of Cv and Ca -- the area-contraction coefficient [12, 13]. The value of Cv is slightly affected by the nozzle inlet shape in this work, as discussed above. It is known that increasing the radius of the corner of nozzle inlet raises the discharge coefficient [14]. Since Ca doesn’t count in the effect of inlet corner shape, neither the product of Cv and Ca. It’s noticed that Cv is calculated from maximum velocity of spray instead of the average velocity in terms of mass flow of the spray. It’s clear that the discharge coefficient represents mass flow rather than dynamics of jet. Measurement of detailed information of velocity is necessary for understanding spray dynamics.

## References

1. A.G. MacPhee, M.W. Tate, C.F. Powell, Y. Yue, M.J. Renzi, A. Ercan, S. Narayanan, E. Fontes, J. Walther, J. Schaller, S.M. Gruner, and J. Wang, “X-ray imaging of shock waves generated by high-pressure fuel sprays,” *Science* 295:1261-1263 (2002).
2. Y. Wang, X. Liu, K.-S. Im, W.-K. Lee, J. Wang, K. Fezzaa, D.L.S. Hung, and J.R. Winkelman, “Ultrafast x-ray study of dense-liquid-jet flow dynamics using structure-tracking velocimetry,” *Nature Physics* 4:305-309 (2008).
3. Z. Liu, K.-S. Im, X. Xie, Y. Wang, K. Fezzaa, M.-C. Lai, and J. Wang, “Single-shot ultra-fast phase-contrast x-ray imaging of high-pressure diesel fuel sprays,” *Energy Materials in the Merged-Flame Regime*, *Eleventh Triennial International Conference on Liquid Atomization and Spray Systems (ICLASS)*, Vail, Colorado USA, July 2009.
4. S.W. Wilkins, T.E. Gureyev, D. Gao, A. Pogany, and A.W. Stevenson, “Phase-contrast imaging using polychromatic hard X-rays,” *Nature* 384: 335–338 (1996).
5. R.J. Adrian, “Twenty years of particle image velocimetry,” *Experiments in Fluids* 39: 159-169 (2005).
6. D.L. Sedarsky, M.E. Paciaroni, M.A. Linne, J. R. Gord, and T.R. Meyer, “Velocity imaging for the liquid–gas interface in the near field of an atomizing spray: Proof of concept,” *Opt. Lett.* 31: 906–908 (2006).
7. K.-S. Im, K. Fezzaa, Y. Wang, X. Liu, and J. Wang, “Particle tracking velocimetry using fast x-ray phase-contrast imaging,” *Applied Physics Letters* 90, 091919 (2007).

8. A.L. Kastengren, C.F. Powell, T. Riedel, S.-K. Cheong, Y. Wang, K.-S. Im, X. Liu, and J. Wang, "Improved Method to Determine Spray Axial Velocity Using X-Ray Radiography", *20th Annual Conference on Liquid Atomization and Spray Systems*, Chicago, IL, May 2007.
9. A.L. Kastengren, C. F. Powell, T. Riedel, S. -K. Cheong, Y. Wang, K. -S. Im, X. Liu, J. Wang, "Determination of Diesel Spray Axial Velocity Using X-Ray Radiography" *Society of Automotive Engineers, Paper 2007-01-0666*.
10. Z. Liu, K.-S. Im, Y. Wang, K. Fezzaa, X. Xie, M.-C. Lai, and J. Wang, "Near-Nozzle Structure of Diesel Sprays Affected by Internal Geometry of Injector Nozzle: Visualized by Single-Shot X-ray Imaging," *Society of Automotive Engineers, Paper 2010-01-0877*.
11. J.B. Heywood, *Internal combustion engine fundamentals*, McGraw-Hill Science/Engineering/Math, 1<sup>st</sup> Edit, 1988, PP. 906-907.
12. J.D. Naber and D.L. Siebers, "Effects of gas density and vaporization on penetration and dispersion of diesel sprays", *Transactions of the SAE*, Vol. 105, Sect. 3, pp. 82-111, 1996.
13. D.L. Siebers, "Scaling liquid-phase fuel penetration in diesel sprays based on mixing-limited vaporization", *Transactions of the SAE*, Vol. 108, Sect. 33, pp. 703-728, 1999.
14. T.R. Ohm, Dwight W. Senger, and Arthur H. Lefebvre; "Geometric effects on spray cone angle for plain-orifice atomizers," *Atomization and Sprays*, vol. 1 n.2, pp. 137-153, 1991.

#### **Notice of Current Address**

Kyoungsu Im: Livermore Software Technology Corp., Livermore, CA 94551 USA

Yuejie Wang: Shanghai Jiao Tong University, China.

#### **Acknowledgments**

This work and the use of the APS at Argonne National Laboratory were supported by the U. S. Department of Energy (DOE), Office of Science, Office of Basic Energy Sciences, under Contract No. DE-AC02-06CH11357. The work is partially supported by DOE Office of Vehicle Technology.